Hindawi
Journal of Sensors
Volume 2021, Article ID 2483518, 11 pages
https://doi.org/10.1155/2021/2483518

Research Article

Research on X-Ray Inspection of Basin Insulators and Wireless Image Sensing Technology

Chunjiang Yan and Liuxue Zhao

State Grid Beijing Electric Power Company, Beijing 100031, China

Correspondence should be addressed to Chunjiang Yan; ycjjj888@163.com

Received 1 September 2021; Revised 19 September 2021; Accepted 20 September 2021; Published 26 October 2021

Academic Editor: Guolong Shi

This paper presents an in-depth study and analysis of X-ray inspection of basin insulators by wireless sensing technology. Aiming at the characteristics of low contrast and many kinds of noise in the basin insulator ray image, this paper proposes an X-ray basin insulator image denoising method based on improved 3D block matching. Using the RF microcontroller CC2530 chip as the core hardware and networked by ZigBee protocol, the sensor senses and collects various parameters and transmits this information to the monitoring end in real time through wireless. The method proposes an improved wavelet thresholding denoising method to overcome the pseudo-Gibbs phenomenon caused by the wavelet hard thresholding method in the 3D block matching algorithm cofiltering and retain more details of the image. Aiming at the ringing effect caused by the Wiener filtering method used in the three-dimensional block matching algorithm collaborative filtering, an improved Kalman filtering method based on anisotropic diffusion is proposed, which avoids the ringing effect, and has clear edges and complete details. An improved Kalman filtering method based on anisotropic diffusion is proposed to avoid the ringing effect, and the edges are clear, and the details are complete. The proposed method is a safe, efficient, accurate, and feasible method for detecting defects in basin insulators by combining X-ray and improved wireless image sensing technology to detect the internal equipment without disassembling or touching the GIS equipment.

1. Introduction

The basin insulator is an important part of the GIS that supports the busbar and isolates the gas chamber and is critical to the safety of the entire equipment. The pot insulator is a composite material made of epoxy resin and alumina. The production temperature and process curing may cause inconsistent differentiation of the two materials, resulting in significant differences in internal stresses and serious cracks or bubble defects after high pressure is added, while foreign object defects may be formed when some of the metals fall off or the equipment ages during installation and use [1]. In recent years, among the factors causing GIS failures, the proportion of outage accidents caused by basin insulator failures has been increasing and often resulting in serious accidents. The special material of the basin insulator and the particularity of its installation location led to defects that are difficult to be detected in advance, causing huge losses to the company and the country after an accident. Seeking a method that can detect the internal state of power equipment without disassembling the equipment, i.e., achieving fault detection with maximum savings on various expenses, is an effective means to ensure the safe and reliable operation of the power grid [2]. Continuous wavelet transform, discrete binary wavelet transform, and wavelet coefficient expansion are closely related to each other. Among them, the discrete binary wavelet transform used by us for image signal processing is the discrete binary wavelet transform. The use of X-ray visual NDT technology for monitoring the operating status of power equipment is an electric detection method developed in recent years that does not require contact, and this method can be used to obtain information on the internal structure of GIS equipment without

disassembling or destroying it. Although the application of this method in the detection of the internal state of substation equipment is still relatively small, based on the multiple advantages of X-ray nondestructive testing makes it develop rapidly in the detection of the internal state of electrical equipment, it has a reliable application prospect and has also become the current research hot spot of nondestructive testing.

With the rapid development of information technology, the high combination of digital electronics and wireless communication technology has realized multifunctional sensor nodes with relatively small size and low power consumption [3]. These tiny sensor nodes are composed of sensing components, data processing components, and communication components, and communication between nodes is nonblocking over short distances, and many nodes can work together using a sensor network approach. Wireless sensor network technology emerged as early as the 1970 s, when the sensor network was composed of sensor nodes and sensing controllers, using point-to-point transmission, and the nodes transmitted data directly to the sensing controllers, which was the prototype of the first generation of sensor networks. Wireless sensor networks are widely used in the military, health, and security fields. Countries all over the world attach great importance to sensor network technology and have invested a lot of researchers and materials to develop various sensor network systems, such as naval collaborative warfare systems and antiterrorism systems. In health, sensor nodes are placed on suitable parts of the patient's body so that the nodes can periodically detect the patient's body information sent to the monitoring center and the doctor can monitor the patient at a remote location, which not only makes it more convenient for the patient but also allows the doctor to better understand the patient's current condition [4]. Sensor network technology is also widely used in the environment, usually for detecting foreign chemicals, air, and water, and can help determine the type, concentration, and location of contaminants, among others [5]. Wireless sensor network technology provides users with intelligence and a good living environment and will become an integral part of our lives in the future. The BM3D method can remove noise better than the previous two methods, but the edges are blurry, and the cracks in the shadow parts are still unclear, and the method in this paper can remove the noise well. Although sensor networks are becoming increasingly widely used, there is a general problem of high-power consumption and high cost of system operation, which gives rise to a new low-power, low-rate, and low-cost short-range wireless communication technology, namely, ZigBee technology [6].

The stresses present in basin insulators are only detected when they accumulate to the point of forming cracks, at which point the insulator needs to be replaced, or the cracks are not detected in time during routine operational inspections, and insulation failures may subsequently occur, which can result in huge economic losses. If stresses can be detected before they accumulate to form cracks, insulation failures can be avoided. Therefore, the use of stress detection values to judge the mechanical properties of insulators and to detect stress abnormalities as early as possible is important for preventing insulator cracking, avoiding insulation failures, and improving the operational safety of GIS insulators. For the case of single routing, the overall, hardware and software parts of the system are designed, respectively, where the hardware part mainly includes hardware selection, terminal nodes, and routing nodes, and the software part mainly includes coordinator, terminal nodes, routing nodes, gateway, and monitoring website. Secondly, a specific wireless sensor network monitoring system is built, and the prediction of the system routing node dormancy time and dynamic duty cycle are tested, respectively, to verify its correctness.

2. Current Status of Research

At present, there are mainly experimental and simulation methods to study the defects of GIS and pot insulators. Experimentation mainly includes preventive outage test and energized inspection test, which can provide a more intuitive and effective understanding of the impact of defects on various aspects of equipment performance, but the experimental cost is relatively high, the conditions are more demanding, and the operation is more cumbersome. In contrast, the simulation analysis method is not as direct as the experimental data but can provide greater convenience for defect research. For the simulation analysis of GIS, many scholars choose to adopt the finite element method. The finite element analysis method, which is continuously improved and optimized based on computer knowledge and numerical analysis, provides a feasible means for many engineering tedious analytical calculations. Nagy et al. investigated the local discharge characteristics of artificial microdefects such as cracks, voids, and delamination generated using precise production control and demonstrated the effect of defects on insulator performance [7]. Zhan et al. proposed to first use the cubic background of the weld image to be detected is simulated by curve fitting, and the simulated background image is numerically subtracted from the original weld image to obtain a weld image with a more uniform background grayscale distribution and a higher detail of defect information, and finally, an appropriate threshold is selected to extract and segment the defects in the weld image [8]. The method is effective in extracting relatively obvious defects to a certain extent, but it is not effective in extracting defects of complex shapes. Moreira et al. proposed a morphology-based welding defect boundary detection algorithm, which first uses reasonable thresholding to improve the effectiveness of the Canny operator for the extraction of defect boundaries [9].

Wireless sensor network technology has achieved good results not only in agriculture but also in medical monitoring, social security, smart home, supermarkets, etc. In cancer treatment, ZigBee technology and QCM immune sensor are used to form a wireless sensor network system [10]. The sensor measures the output frequency of the QCM and transmits the frequency data wirelessly to the coordinator through the ZigBee network, and the coordinator then transmits the received frequency data to the computer for analysis and processing through the serial port [11]. When the house is invaded, the wireless sensor network intrusion monitoring system composed of ZigBee and sensors can alert the house owner through the system by monitoring the link quality value between the coordinator and the terminal node in a closed room is constant,

and if the value changes, it means the house is invaded [12]. Wireless sensor network low-power technology has been in a very important position in the research of wireless sensor network technology along with the development of wireless sensor network systems. At present, wireless sensor network low-power technology has been deeply researched at home and abroad, most of which are researching and optimizing the protocol stack technology [13]. For example, the S-MAC protocol is a contention-based MAC layer protocol for sensor networks that focuses on three aspects, namely, periodic listening and sleep, conflict and crosstalk avoidance, and long message delivery, to reduce the energy consumption of the system while supporting good scalability and conflict avoidance, but its use of adaptive listening and periodic sleep leads to reduced system throughput and increased latency [14].

Various image processing methods have different advantages and disadvantages and need to be reasonably selected and improved according to the actual characteristics of the image when applied, to achieve better processing results. Substations, power plants, and other sites where there is a lot of noise, and because the power equipment is relatively large, the internal structure is very complex, etc., the X-ray digital image is often not ideal, the image is not clear enough, and power equipment image localization, etc. may cause professionals to misjudge the defects. Therefore, the original image must be properly processed to reduce misjudgment and increase the accuracy and reliability of defect identification.

3. Wireless Basin Insulator Image Sensing X-Ray Inspection Technology Design

3.1. Wireless Image Sensing X-Ray Detection Analysis. Wireless sensor networks consist of three parts: sensor nodes, aggregation nodes, and task management nodes. These three parts assume different roles in the infinite sensing network, respectively, and play a decisive role in the function of the wireless sensing network. In the wireless sensing network structure, the number of sensor nodes does more. And in terms of the roles and functions of the different parts, the sensor nodes are the basic components, the aggregation nodes are the information intermediaries and processors, and the task management nodes are the final information adjudicators. Statistics and analysis of the test results of the three parts are carried out to ensure the rationality of the abovementioned low power consumption method and the stability of the system. Given whether the method of introducing the queuing theory model to predict the local optimal sleep time of routing nodes is feasible or not. Specifically, the so-called wireless sensor network is also composed based on these sensor nodes placed in different areas and locations. These sensor nodes can collect the corresponding information of the detected area and realize the transmission and sharing of information with the help of other nodes, to realize the real-time dynamic supervision of the whole monitoring area. After the sensor nodes share the monitoring information at a certain stage, they will realize the statistics and processing of the information through the aggregation node, and finally, the aggregation node will relate to the task management node in series to realize the management and control of the wireless sensing system and ensure the information transmission is error-free.

In this structure, for sensor nodes, the most important thing is the design of their software and hardware, which directly determines the function and realization of the whole wireless sensor network; for aggregation nodes, they require high data processing, statistics, and transmission functions, to be able to communicate the monitoring information thoroughly; for task management nodes, what is more, important is the analysis, calculation, and operation functions, which should be stable, reliable, and efficient. Only when these three parts meet the requirements, the entire wireless sensor network can remain stable and finally play the role of real-time monitoring of the water environment. The time is between 6-7 seconds and 7-8 seconds, which shows that the routing node can sleep after only 8 seconds of work. It also proves that it is feasible for the routing node to sleep with the maximum sleep time estimated by the queuing theory model. Therefore, in the design of this paper, we focus on the software and hardware design of sensor nodes, aggregation nodes, and task management nodes and choose the equipment and materials with high durability and stability as much as possible under the economic condition. The main function of wireless sensor network nodes is the collection and processing of information and the transport and transmission of the collected and processed information. Based on this, the wireless sensor network node is composed of four parts, which are a sensor module, a processor module, a wireless communication module, and an energy supply module, as shown in Figure 1.

Referring to the above diagram, the four modules are in turn composed of several transmitters, some of which are used for internal information transmission and processing, while others are used for external information collection and storage. However, in these three modules, each assumes different roles: the sensor module is mainly responsible for the collection and processing of information in the area to be monitored; the main function of the processor module is to ensure that the communication and transmission of information will not deviate and fail to ensure the stability and reliability of the information transmission process; the main function of the wireless communication module is to communicate and transmit information, which is the main goal of the whole infinite [15]. The power consumption of the routing node after working for 9 hours is 0.23 V. Under normal circumstances, the minimum voltage to supply power to the routing node is 6 V, and the initial voltage of the lithium battery is 12 V, so the routing node can be used continuously for about 10 days. The main function of the wireless communication module is to communicate and transmit information, which is the main goal of the whole infinite network system and the basis of its function. In addition, the energy supply module, as the name implies, is mainly responsible for providing power in the entire wireless sensor network node to ensure that the wireless sensor network operates with sufficient power and all functions work well. In this paper, the design and arrangement of network nodes will be combined with algorithms to calculate the optimal number of network sensors placed in the area to

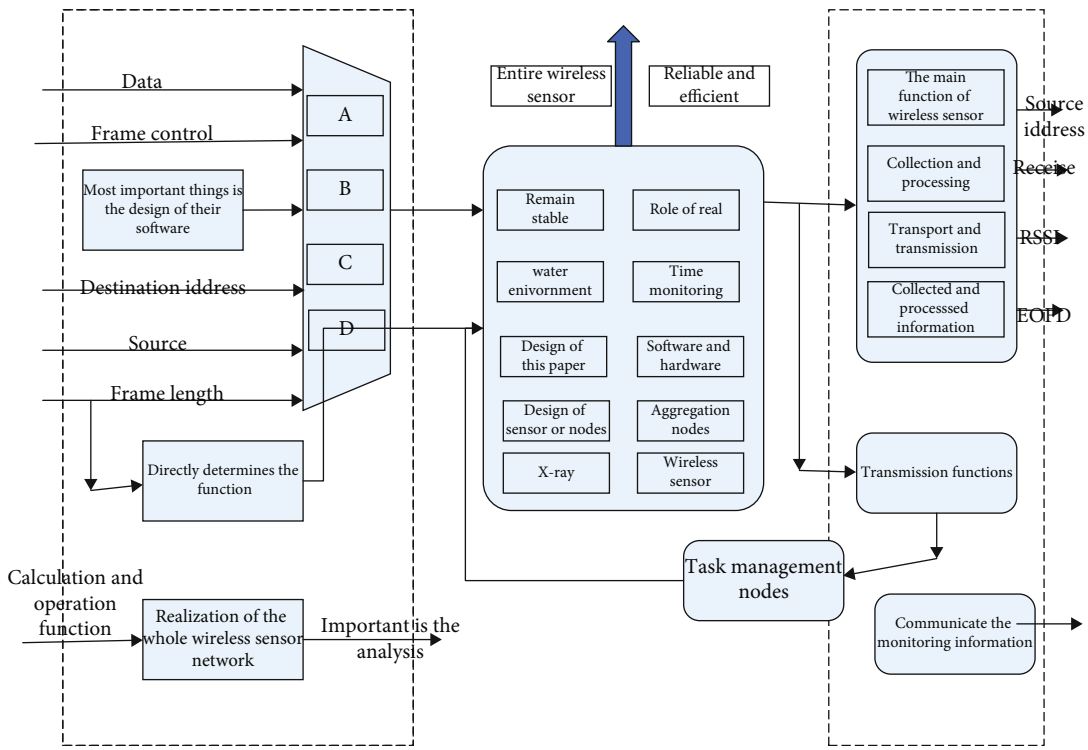

Figure 1: The four main modules of a wireless sensor network node.

ensure the adequacy of information collection and will ensure the smoothness and stability of each network node as much as possible.

The main reference indicators for the selection of X-ray tube in the actual inspection are power and focus; the power size is mainly determined by the thickness of the workpiece size; the focus size will affect the imaging quality and imaging area, according to the characteristics of the product to be tested to select a suitable X-ray tube. The high voltage generator of the X-ray source provides filament voltage and acceleration voltage for the X-ray tube. Based on the high voltage output characteristics of the generator, it can be divided into industrial frequency transformers, medium/high-frequency transformers. The X-ray penetration is the basis of X-ray imaging detection. X-rays pass through the object to be detected, and some photons do not react with the object and directly transmit out, while some photons interact with the object, and a certain degree of attenuation occurs, which results in different imaging effects [16]. The reduction of X-ray intensity by absorption and scattering is called absorption attenuation and scattering attenuation. Absorption is the complete conversion of the photon energy into other energy by the object, and scattering is the partial attenuation of the photon energy due to the change of propagation direction when it passes through the object.

The Line Array Detector (LDA) is a hardware device that converts X-rays into a separated, single-row analog signal of a size proportional to the intensity of the rays in the area, which is then converted to a digital signal by A/D and sent to a computer system for real-time imaging. With adjustable integration time and a very high frame rate, LAD is commonly used in high-speed environments such as defect detection of specially shaped castings (e.g., cylindrical workpieces) and assembly line-item detection.

The initial Mohr streak image acquired by the detector needs to go through a series of image processing algorithms to obtain an image with distinctive features. When the Mohr streak image is acquired by the X-ray wavefront detection device, a series of image processing work is needed for the initial Mohr streak image. For this purpose, a complete image processing process is developed in this paper: illumination inhomogeneity correction algorithm, filtering and denoising algorithm for Mohr streak, image key information enhancement algorithm, threshold segmentation algorithm, and Mohr streak refinement algorithm. In the following, I will introduce these algorithms in detail. By introducing these Moiré stripe image processing algorithms, we can also know the information characteristics of Moiré stripe and extract useful information from Moiré stripe. Figure 2 shows a series of image processing workflow after the original image is acquired from the X-ray detector.

We know that in the image with uniform light distribution, the light distribution in the two-dimensional space is relatively uniform, so the intensity of each position of this image is maintained all the time, so the overall effect of the image is better, and the image performance is very natural. However, in the image with uneven light distribution, the intensity of each position is not necessarily the same, and the intensity of some positions may be too strong, and some positions may be too weak, so the image with uneven light distribution affects the next experiment, and the internal details of the image are not shown, which affects the researchers' observation and judgment.

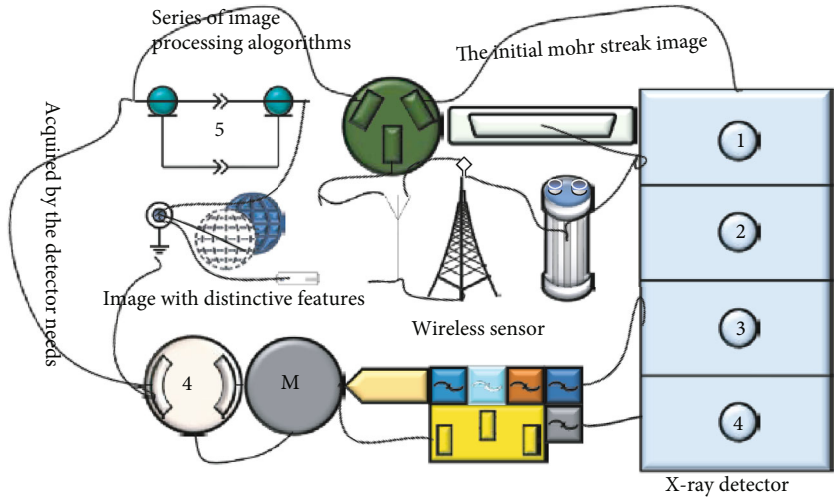

Figure 2: Wireless image sensing X-ray detection framework.

The X-ray image acquired by an X-ray real-time imaging system is a digital image. In the field of electronic imaging, a two-dimensional function $f(x, y)$ is used to define an image. According to the mathematical definition, the value or magnitude off at the spatial coordinates (x, y) is a positive scalar whose physical meaning is determined by the image. X-ray images are generated by imaging systems in which, according to their basic principles, the intensity of the brightness on the image is proportional to the energy of the X-rays passing through the object. Since the data sensed by the optical sensor is a continuous voltage waveform, the digital image generated by the control system through sampling and quantization of a continuous image represented by $f(x, y)$ is converted into a digital image consisting of a finite number of discrete points in an ordered arrangement.

$$f(x,y) = \begin{bmatrix} f(0,0) & f(0,1) & \cdots & f(0,N) \\ f(1,0) & f(1,1) & \cdots & f(1,N) \\ \cdots & \cdots & \cdots & \cdots \\ f(M,0) & f(M,1) & \cdots & f(M,N) \end{bmatrix}, \quad (1)$$

$$P(z) = \frac{2}{\sqrt{2\pi\sigma}} \exp\left(z - \mu^2\right)^2.$$

The actual transmission range between two nodes is usually between ten and one hundred meters. This can be increased to a thousand to three thousand meters by increasing the transmitting power of the radio frequency, which enables the relaying of the communication through the nodes of the router. The transmission distance can theoretically reach twice the network depth of the network depth × the distance between the two token nodes that can be covered [17]. In this case, the network node can automatically sense the presence of other nodes and confirm its connection status with them to build a structured network with them. And when a node in the network has a breakpoint, failure, blockage, or a change in node location, the network can repair itself and make the network topology a stage.

3.2. Basin Insulator Image Processing. Due to the variety and random distribution of X-ray image noise, this paper proposes a new method for X-ray basin insulator crack identification based on an improved three-dimensional block matching image denoising method. To avoid the pseudo-Gibbs phenomenon caused by the wavelet hard thresholding method in the cooperative filtering of the 3D block matching algorithm, an improved wavelet thresholding denoising method is proposed, which not only avoids the influence of the pseudo-Gibbs phenomenon but also allows more image details to be retained [18]. The production temperature and process solidification will cause the aggregation and differentiation of the two materials to be inconsistent, resulting in obvious internal stress differences. Cracks or bubble defects will form when the high pressure is severe. At the same time, part of the metal falls off or equipment during installation and use. Aging may also form foreign body defects. In response to the "ringing effect" caused by the Wiener filtering method in the 3D block matching algorithm, an improved Kalman filtering method based on anisotropic diffusion is proposed, which avoids the ringing effect, and the edges are clear, and the details are complete. The method can greatly suppress image noise and improve the quality of X-ray images, which lays a good image foundation for subsequent fault identification and greatly improves the accuracy of fault identification.

The quality of basin insulator radiographic images directly affects the accurate identification of the location, size, and type of defects in basin insulators. X-ray images are often contaminated by a variety of noises due to the interference of the imaging environment inside the X-ray machine and the external environment during their acquisition, transmission, and recording. The presence of noise can drown the important information features in the image in

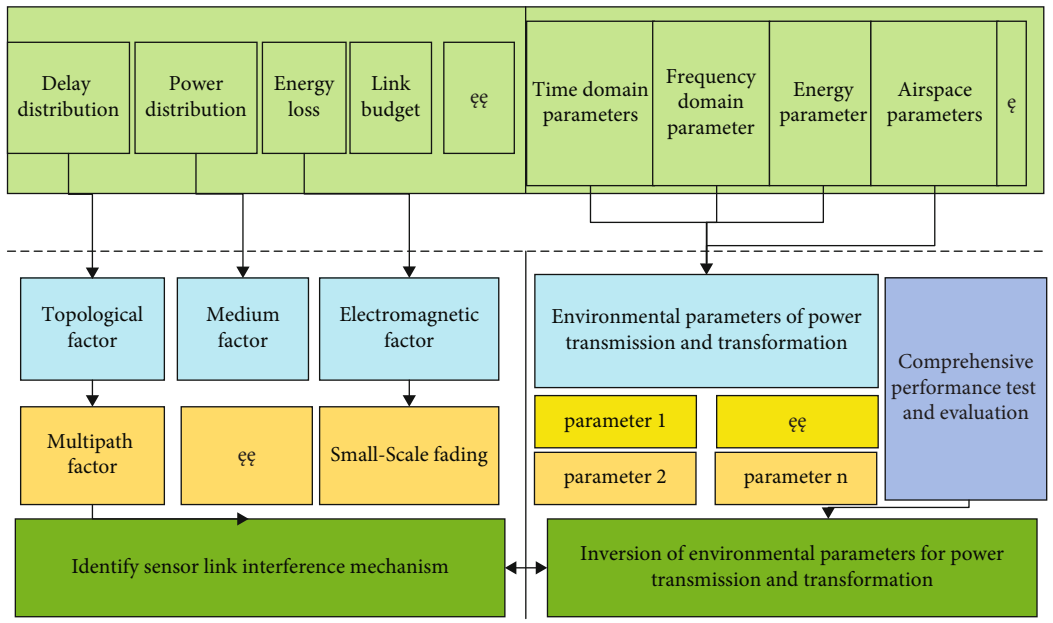

Figure 3: Flow chart of algorithm framework.

noise, causing image degradation and affecting the visual effect of the image and the accurate identification of faults. X-ray through the object can be imaged mainly related to the material of the object, and the greater the density, the more the ray attenuation, and thus the less the residual dose of radiation. X-ray image generation process, during the emission of electrons from the cathode of the radiation machine and the microchannel plate electron multiplication, will cause up and down the noise; the fluorescent screen outward photon generation may not only cause up and down the noise, but also cause particle noise; in addition, there is the CCD image acquisition thermal noise, etc. Therefore, the X-ray image noise shows a Gaussian distribution in the probability distribution and a white noise characteristic in the power spectrum, while small cracks, bubbles, and other faults are often easily covered by noise and cannot be identified [19]. Therefore, it is necessary to effectively denoise the X-ray basin insulator images, as shown in Figure 3.

The wavelet transform image denoising method is a time-frequency analysis method that can combine the features of time and frequency domains and is widely used because it has the characteristics of multiscale analysis. The wavelet transform can process signals from coarse to fine. Wavelet transform is a method of image denoising with the same basic idea as the conventional Fourier Transform, which is an orthogonal or nonorthogonal transform within a limited width. The wavelet transform is a function or image signal represented by a family of functions, the family of functions that is the wavelet function family. The wavelet function system is formed by a basic wavelet function through a certain transformation, where its basic function to meet in the frequency and position can be varied, and such a wavelet function in the finite width of the waveform is called wavelet. Wavelet transform includes continuous wavelet transform, discrete binary wavelet transforms, and wavelet coefficient expansion, which are closely related to each other, among which the discrete binary wavelet transform was used for image signal processing.

$$w_\lambda = \begin{cases} \text{sign } (w + \lambda) \\ 1 \end{cases}. \tag{2}$$

The method considers both the image and noise as smooth random signals and uses the minimum mean square error criterion to solve for the optimal filter parameters.

$$X(u, v) = \frac{X(u, v)^2}{X(u, v)^2 - \lambda^2} Y(u, v). \tag{3}$$

The key to X-ray image fault identification is whether the details of the fault are prominent or not. The purpose of denoising is to suppress the noise and highlight the details of the image, to better identify the crack boundary, so a method is needed to remove the noise interference while preserving the complete crack boundary. To make up for the above shortcomings of Wiener filtering, an improved Kalman filtering method based on anisotropic diffusion is proposed as a secondary denoising method in the BM3D method, which can effectively avoid the "ringing effect" and make it more suitable for denoising X-ray images. The realization of fault detection is an effective means to ensure the safe and reliable operation of the power grid. The use of X-ray visual nondestructive testing technology to monitor the operating status of power equipment is a noncontact live detection method developed in recent years. This method can be used for GIS equipment without disassembling and damaging the GIS equipment. Transillumination was used to obtain internal structure information.

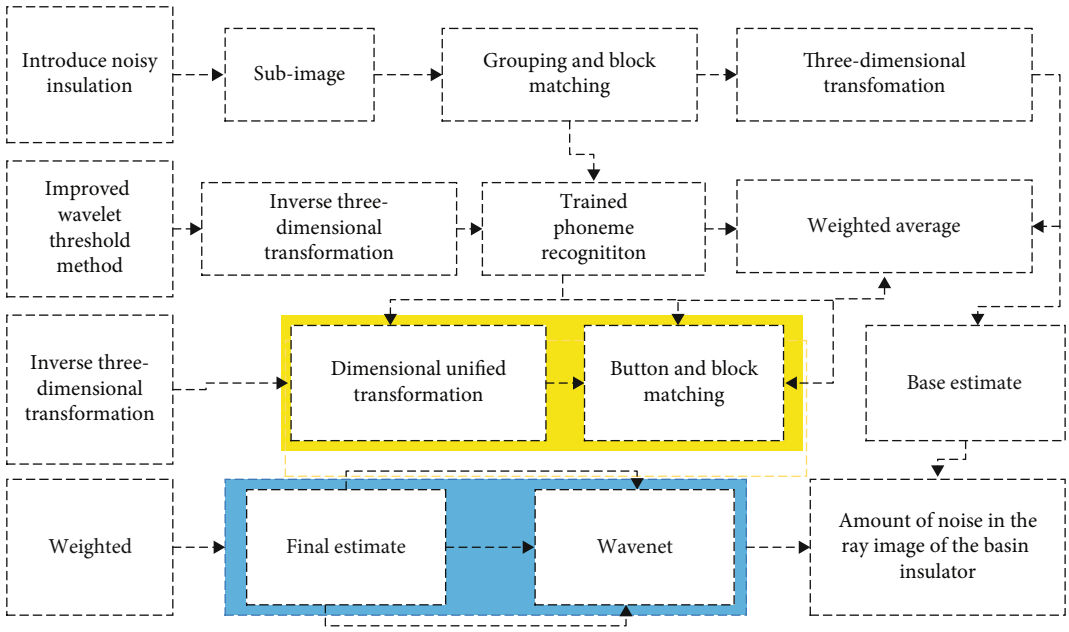

Figure 4: Graphical processing flow.

The key to X-ray image fault identification is whether the details of the fault are prominent or not. The purpose of denoising is to suppress the noise and highlight the details of the image, to better identify the crack boundary, so a method is needed to remove the noise interference while preserving the complete crack boundary.

$$f(a,b) = \sum_{R} \beta_{kl} f(a+k, b+l) - n(a,b). \tag{4}$$

The above Kalman filtering can filter out most of the noise, but this method uniformly filters all pixels of the whole image, which tends to blur the edges for low-contrast, noisy X-ray images. In this paper, an improved Kalman filtering method based on anisotropic diffusion is proposed based on the existence of both high-contrast boundaries and uniformly wide regions in the middle of the X-ray image of a pot insulator. After the above two improvement steps, the flow of the improved 3D block matching algorithm in this paper is shown in Figure 4.

There is a large amount of noise in the ray image of the basin insulator, which makes the crack fault information drowned in the noise and difficult to identify. The wavelet hard thresholding method does not remove the noise completely, there are a lot of noise points staying in the figure, and the edges are blurred, and the cracks are almost invisible in the shadow parts; the Wiener filtering method removes the noise better than the wavelet hard thresholding, but there are still noise residues, and the noise removal effect in the shadow parts is not obvious; the BM3D method removes the noise relatively better than the first two methods, but the edges are blurred, and the cracks in the shadow parts [20]. The BM3D method has better noise removal than the previous two methods, but the edges are blurred, and the cracks in the shadow areas are still not clear, while the method in this paper not only has good noise removal but also highlights the image details, so that the cracks in the shadow areas can be presented, which is a more ideal denoising method.

The residual image of the wavelet hard thresholding method shows a certain pattern, with black dots in the middle and white dots in the periphery, indicating that there is little noise in the residual image, which means that the noise removal is not complete and the quality of the image is improved very little after denoising; the residual image of the Wiener filtering method has obvious circles and crack curves, indicating that the Wiener filtering method removes a lot of useful information of the edges in the denoising process, and the denoising is excessive. These tiny sensor nodes are composed of sensing components, data processing components, and communication components. The communication between the nodes is nonblocking within a short distance, and many nodes can use the sensor network to work together. The residual image of the BM3D method has a vague circular outline in the middle, which means that the edge information of the image is removed during denoising and some useful information is lost, while the residual image of this paper does not have any structure, i.e., there is no obvious figure, and it is randomly distributed, which means that only the noise is removed and the details of the image are retained to the maximum, which again verifies that the denoising effect of this paper is good.

4. Analysis of Results

4.1. Wireless Image Sensing X-Ray Detection Performance Analysis. Based on some applications of queuing theory in routing performance analysis, this paper establishes a theoretical basis for predicting the optimal dormancy time of local

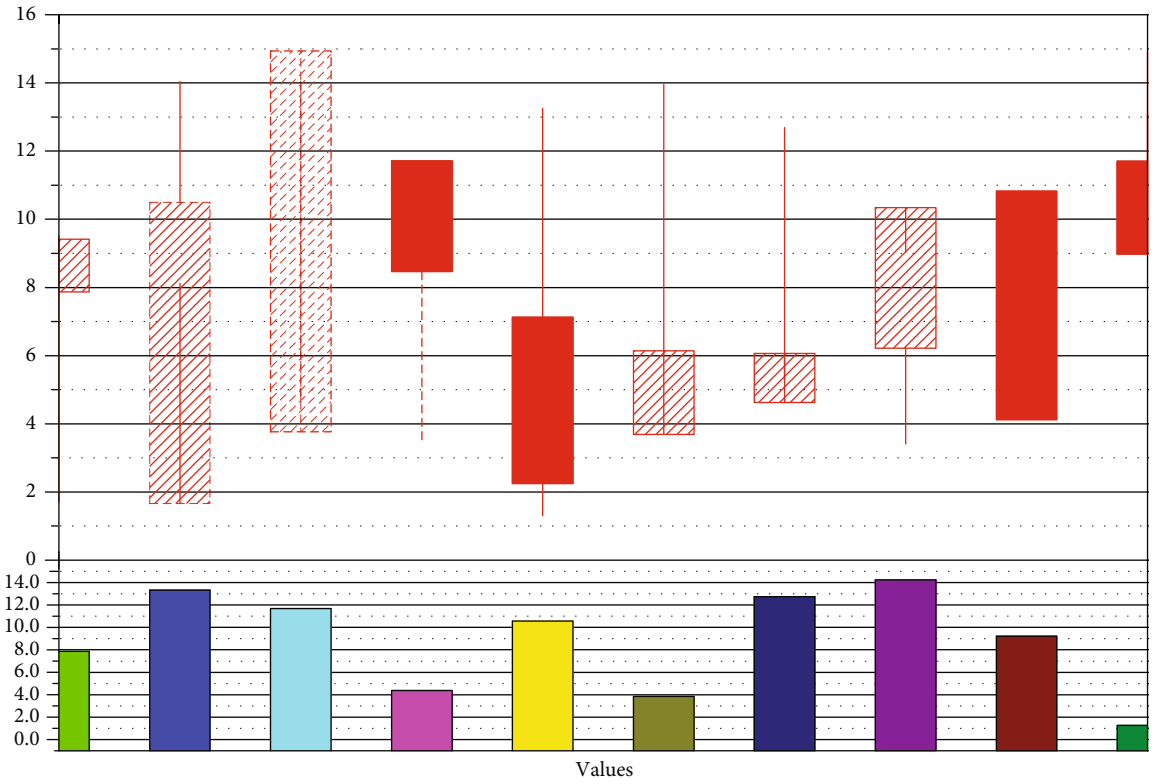

Figure 5: Test results of the prediction method.

routing nodes using the queuing theory model, and on this basis, a dynamic model is built using queuing theory to realize the dynamic duty cycle of routing nodes, which makes the system more stable. In this section, a specific test monitoring system is built to test the feasibility of hibernation by routing nodes using the optimal hibernation time estimated by the queueing theory model, the feasibility of dynamic hibernation by routing nodes using the dynamic hibernation time estimated by the dynamic model of queueing theory, and the power consumption of routing nodes under different hibernation times in three parts. Then, the test results of the three components statistically analyzed to ensure the rationality of the above low-power method and the stability of the system. The feasibility of using the optimal hibernation time estimated by the queueing theory model for routing nodes is tested to determine whether the abovementioned method for predicting the local optimal hibernation time of routing nodes is feasible. This not only makes the patient more convenient but also allows doctors to better understand the patient's current situation. Sensor network technology has also been widely used in the environment. It is usually used to detect foreign chemical reagents, air, and water and can help determine the status of pollutants. Based on the real environment of Cha Shan, the test system also uses a tree network topology with one coordinator, one routing node, and two terminal nodes in the network. In addition, the distance between the coordinator and the routing node and between the routing node and the end node is about 75 meters, and there are walls and other obstructions between the nodes.

Then, the routing nodes were first connected to power, and when the routing nodes were powered up, then the end nodes were powered up in turn. Finally, the system experimented several times for 10 hours, and the number of entries (averaged multiple times) of data received by the coordinator at the end nodes was counted at what time. The predicted test results of the routing node hibernation time are shown in Figure 5.

From Figure 5, after the network synchronization of the system, the coordinator receives the data collected by terminal nodes 1 and 2 within 1 minute (one cycle) between 6-7 seconds and 7-8 seconds, respectively, which shows that the routing nodes can hibernate after working for only 8 seconds and proves that it is feasible for the routing nodes to hibernate using the maximum hibernation time estimated by the queueing theory model. In addition, the coordinator receives 54 data from each of end nodes 1 and 2 in 10 hours with a packet loss rate of 0.091, which is a good application in systems where the packet loss rate is not very demanding.

In practical applications, after the design of the system, the various functional modules of the system need to be tested. Insulators need to be replaced, or cracks are not found in time during routine inspections, and then, insulation failures may occur. The economic losses caused by this are huge. According to the basic principles of specific system testing, the integrity of the system and the practical application should be considered in the process of system operation. The power consumption of the routing nodes is tested for different resting times. Based on the maximum hibernation time calculated above, the hibernation

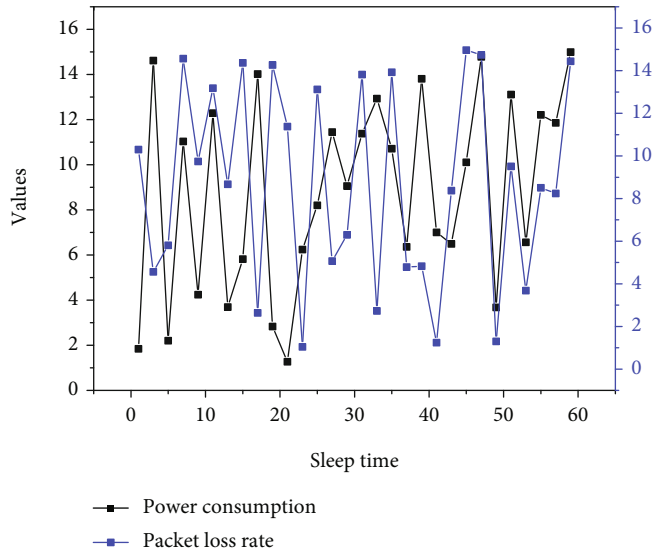

Figure 6: Power consumption and packet loss rate of routing nodes.

time for the routing node is set to 52 seconds, 40 seconds, 30 seconds, 20 seconds, 10 seconds, no hibernation for all six groups, and 52 seconds for the 2 terminal nodes. Under the same conditions, the experiment conducted for 9 hours for these six groups, and the power consumption of each group of routing nodes and the packet loss rate of the terminal nodes are calculated after 9 hours, and the experimental results are shown in Figure 6.

As the hibernation time of the routing node increases, the power consumption of the routing node becomes lower after 9 hours, while the packet loss rate of the routing node increases. The above hibernation method of routing nodes can be used in some monitoring where the packet loss rate is not required. After the sensor nodes share the monitoring information of a certain stage, they will realize the statistics and processing of the information through the sink node, and finally, the sink node and the task management node will be connected in series to realize the management and control of the wireless sensor system to ensure error-free information transmission. The power consumption of the routing node is 0.23 V after 9 hours of operation with a hibernation time of 52 seconds and an interruption time of 1 minute. 6 V is the minimum voltage required to power the routing node under normal conditions, and the initial voltage of the lithium battery is 12 V, so the routing node can be used continuously for about 10 days. If the interruption time is 1 hour, theoretically the routing node can be used continuously for about 600 days. Under the premise of ensuring network stability and data reliability, the routing nodes can extend the network lifetime well by using the maximum sleep time estimated by the queueing theory model for sleep. Secondly, the dynamic hibernation of routing nodes using the maximum hibernation time estimated by the queueing theory dynamic model can solve the problem caused by the change of the number of terminal nodes of the system, which further increases the stability of the system.

4.2. Wireless Pot Insulator Image Detection Results. A series of radiographic images of basin insulators with image size $2048 * 2048$ were acquired by the device in Figure 7. A part of the images, including 250 images of cracks, 250 images of bubbles, 250 images of foreign objects, and 125 images without defects, were selected for image recognition. Using these images alone as training data for CNN was not enough, so each image was rotated in 8 directions and compressed to $28 * 28$ images to get 8 images through one image. After the processing, the image library was expanded from the original 875 images to 7000 images. From these, 250 images of each category are randomly selected, totaling 1000 images as test samples and the remaining 6000 images as training samples. Of course, the training library still needs to be expanded in future practice to improve the defective images and make the recognition results more accurate. More important are the analysis, calculation, and operation functions, which must be stable, reliable, and efficient. Only when these three parts meet the requirements can the entire wireless sensor network remain stable and ultimately play the role of real-time monitoring of the water environment. For the limitation that the traditional convolutional kernel can only see the features in the fixed area and fixed shape range, this paper proposes a deformable convolutional kernel, and the deformed convolutional kernel can see more regions of interest, which makes the recognized features more perfect and typical, as shown in Figure 7.

The overall recognition accuracy of the improved CNN algorithm in this paper is higher than that of the traditional CNN algorithm, and the convergence speed is faster. The improved CNN algorithm in this paper converges to 100% recognition accuracy after 25 iterations, while the traditional CNN algorithm converges to 100% accuracy after 35 iterations. The algorithm in this paper has a faster convergence speed and higher accuracy than the traditional algorithm.

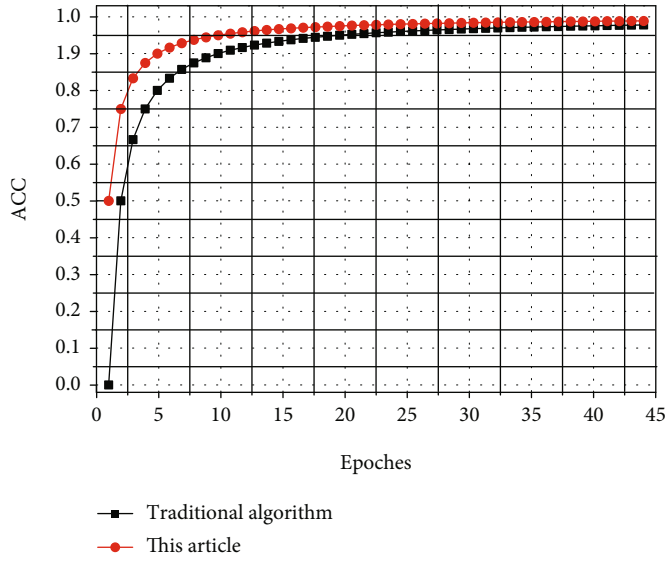

Figure 7: Effect of the number of iterations on recognition performance.

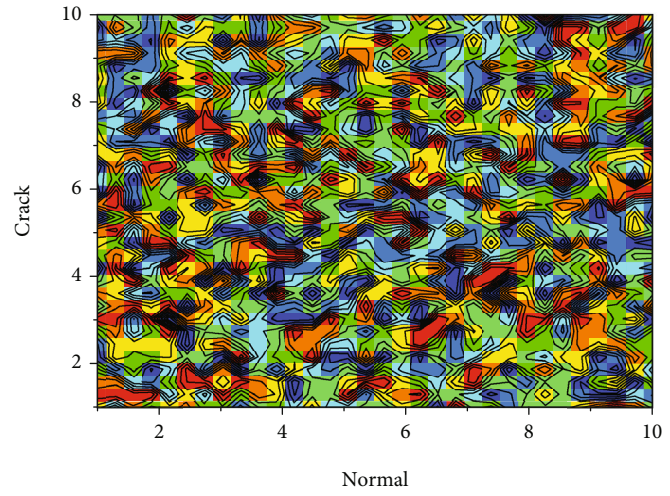

Figure 8: Test defect identification results.

From Figure 8, it can be seen that for normal images, the recognition rate is as high as 100% because of the uniform recognition; for images with defects, the recognition rate decreases due to the size of defects and different materials, and crack defects generally have a certain length and are better recognized, with an accuracy rate of 99.6%; bubble defects have a small area and are not easily recognized, with an accuracy rate of 98.8%; the recognition rate of foreign object defects is relatively low, 98.0%. This is mainly related to the material of the foreign object, which has different transmission rates of different materials to the rays, which will lead to different imaging differences. Weakening the intensity of X-rays through absorption and scattering is called absorption attenuation and scattering attenuation. Absorption mainly means that the energy of the photon is completely received by the object and converted into other energy and attenuated and disappeared. Scattering refers to the attenuation of part of the energy when the propagation direction of the photon passes through the object is changed. Overall, the improved CNN method has a recognition rate of 98% or more for defects, which applies to most of the defect detection and has some practical value.

Using the residual image and PSNR as the performance indicators of the denoising algorithm, we compare the denoising effect of the proposed improved 3D block matching denoising method with the wavelet hard thresholding, Wiener filtering, and BM3D algorithms.

5. Conclusion

In this paper, the results after data aggregation and analysis can be counted and summarized, and the structural design

of the water environment monitoring system based on ZigBee wireless sensing technology is described, focusing on four major parts: its system framework, network structure, data acquisition system design, and data collection system design. In this paper, a basin insulator ray image denoising method based on improved 3D block matching is proposed. For the pseudo-Gibbs phenomenon caused by the wavelet hard thresholding method in the 3D block matching algorithm cofiltering, an improved wavelet thresholding denoising method is proposed, which not only avoids the influence of the pseudo-Gibbs phenomenon but also allows more image details to be preserved; for the "ringing effect" caused by the Wiener filtering method in the 3D block matching algorithm cofiltering, an improved wavelet thresholding method is proposed. In response to the "ringing effect" caused by the Wiener filtering method in the 3D block matching algorithm, an improved Kalman filtering method based on anisotropic diffusion is proposed, which avoids the ringing effect, and the edges are clear, and the details are complete. From the denoising image comparison, it can be seen that the method proposed in this paper greatly suppresses the image noise; from the residual image comparison, it can be seen that the method in this paper not only retains the image detail basis, but also suppresses the noise well. The accuracy of fault identification is greatly improved.

Data Availability

The data used to support the findings of this study are included within the article.

Conflicts of Interest

All the authors do not have any possible conflicts of interest.

Acknowledgments

This study was supported by the State Grid Beijing Electric Power Company.

References

[1] C. Xu and G. Zhu, "Intelligent manufacturing lie group machine learning: real-time and efficient inspection system based on fog computing," *Journal of Intelligent Manufacturing*, vol. 32, no. 1, pp. 237–249, 2021.

[2] N. di Trani, A. Silvestri, A. Sizovs et al., "Electrostatically gated nanofluidic membrane for ultra-low power controlled drug delivery," *Lab on a Chip*, vol. 20, no. 9, pp. 1562–1576, 2020.

[3] S. K. Ghosh, T. K. Sinha, M. Xie et al., "Temperature–pressure hybrid sensing all-organic stretchable energy harvester," *ACS Applied Electronic Materials*, vol. 3, no. 1, pp. 248–259, 2021.

[4] P. Hillger, J. Grzyb, R. Jain, and U. R. Pfeiffer, "Terahertz imaging and sensing applications with silicon-based technologies," *IEEE Transactions on Terahertz Science and Technology*, vol. 9, no. 1, pp. 1–19, 2019.

[5] I. Malhotra, K. R. Jha, and G. Singh, "Terahertz antenna technology for imaging applications: a technical review," *International Journal of Microwave and Wireless Technologies*, vol. 10, no. 3, pp. 271–290, 2018.

[6] Z. Huang, Y. Hao, Y. Li et al., "Three-dimensional integrated stretchable electronics," *Nature Electronics*, vol. 1, no. 8, pp. 473–480, 2018.

[7] B. Nagy, T. K. Simon, and R. Nemes, "Effect of built-in mineral wool insulations durability on its thermal and mechanical performance," *Journal of Thermal Analysis and Calorimetry*, vol. 139, no. 1, pp. 169–181, 2020.

[8] T. Zhan, R. Yamato, S. Hashimoto et al., "Miniaturized planar Si-nanowire micro-thermoelectric generator using exuded thermal field for power generation," *Science and Technology of Advanced Materials*, vol. 19, no. 1, pp. 443–453, 2018.

[9] A. S. B. Moreira, C. A. Silva, and I. A. Silva, "Custom logo MIFARE ultralight EV1 RFID TYVEK wristbands for events-chinayintl. com," *REM-International Engineering Journal*, vol. 71, no. 2, pp. 261–267, 2018.

[10] D. K. Rajak, D. D. Pagar, R. Kumar, and C. I. Pruncu, "Recent progress of reinforcement materials: a comprehensive overview of composite materials," *Journal of Materials Research and Technology*, vol. 8, no. 6, pp. 6354–6374, 2019.

[11] H. Ren, G. Zou, Z. Zhao et al., "High-reliability wireless packaging for high-temperature SiC power device sintered by novel organic-free nanomaterial," *IEEE Transactions on Components, Packaging and Manufacturing Technology*, vol. 10, no. 12, pp. 1953–1959, 2020.

[12] J. Chun, R. A. Kishore, P. Kumar et al., "Self-powered temperature-mapping sensors based on thermo-magneto-electric generator," *ACS Applied Materials & Interfaces*, vol. 10, no. 13, pp. 10796–10803, 2018.

[13] T. Wang, D. Ou, H. Liu et al., "Thermally conductive boron nitride nanosheet composite paper as a flexible printed circuit board," *ACS Applied Nano Materials*, vol. 1, no. 4, pp. 1705–1712, 2018.

[14] I. Se, "Total table of contents in 2020," *International Journal of Agricultural and Biological Engineering*, vol. 13, no. 6, pp. 248–256, 2020.

[15] Q. Wang, C. R. Bowen, W. Lei et al., "Improved heat transfer for pyroelectric energy harvesting applications using a thermal conductive network of aluminum nitride in PMN–PMS–PZT ceramics," *Journal of Materials Chemistry A*, vol. 6, no. 12, pp. 5040–5051, 2018.

[16] S. Mustapha, Y. Lu, C. T. Ng, and P. Malinowski, "Sensor networks for structures health monitoring: placement, implementations, and challenges—a review," *Vibration*, vol. 4, no. 3, pp. 551–584, 2021.

[17] A. S. B. Moreira, C. A. Silva, and I. A. Silva, "Medical disposable needles blood safety Lancet-chinayintl. com," *REM-International Engineering Journal*, vol. 71, no. 2, pp. 261–267, 2018.

[18] M. H. Seo, J. H. Ko, J. O. Lee et al., "> 1000-fold lifetime extension of a nickel electromechanical contact device via graphene," *ACS Applied Materials & Interfaces*, vol. 10, no. 10, pp. 9085–9093, 2018.

[19] Z. Meng, R. M. Stolz, L. Mendecki, and K. A. Mirica, "Electrically-transduced chemical sensors based on two-dimensional nanomaterials," *Chemical Reviews*, vol. 119, no. 1, pp. 478–598, 2019.

[20] J. Luo, L. Wang, X. Huang et al., "Mechanically durable, highly conductive, and anticorrosive composite fabrics with excellent self-cleaning performance for high-efficiency electromagnetic interference shielding," *ACS Applied Materials & Interfaces*, vol. 11, no. 11, pp. 10883–10894, 2019.